ChemComm

Light-Driven Dissipative Self-Assembly of a Peptide Hydrogel

Journal:	*ChemComm*
Manuscript ID	CC-COM-09-2021-004971.R1
Article Type:	Communication

COMMUNICATION

Light-Driven Dissipative Self-Assembly of a Peptide Hydrogel

Mengmeng Liu,[†] Cassidy N. Creemer,[†] Thomas J. Reardon, and Jon R. Parquette*[a]

Received 00th January 20xx,
Accepted 00th January 20xx

DOI: 10.1039/x0xx00000x

Light energy provides an attractive fuel source for energy dissipating systems because of the lack of waste production, wavelength tunability and the potential for spatial and temporal resolution. In this work, we describe a peptide-spiropyran conjugate that assembled into a transient nanofiber hydrogel in the presence of visible light, and dissociated when the light source was removed. The transient nature of the hydrogel permitted cycling between the sol- and gel states by switching the light off and on.

Self-assembly has become a powerful strategy to create nanoscale materials with exceptional properties that are critical to many areas of materials and biomedicine.[1,2] Many of these assembled nanomaterials exhibit features, such as self-healing and responsivity, that are derived from their thermodynamic stability.[3,4] These systems evolve the starting components toward a set of stable structures that persist at a global or local thermodynamic minimum with no net flux of energy through the system.[5] However, the more complex actions of the biological machinery in nature depend on an energy-dependent, dynamic instability in the formation and breakdown of their functional states.[6] Biological systems utilize kinetically controlled structures that reside in non-equilibrium states and require the continuous dissipation of energy to exist and to function.[7] The spatiotemporal control over the system afforded by chemical energy permits these systems to accomplish work such as cell division, motility, transport and muscle contractions. The functional property that emerges from the formation of a transient assembly endures only as long as energy is supplied. Achieving the full potential of molecular assembly to create intelligent, life-like materials requires the design of systems that exist outside the confines of thermodynamic minima.

Accordingly, there has been a considerable drive to design self-assembled systems that continuously dissipate energy, with the expectation that they will have novel properties not accessible with assembled structures that exist only at equilibrium.[8] Most dissipative systems that have been studied rely on chemical energy, in the form of a reagent, to elevate a precursor to a higher energy state that subsequently undergoes self-assembly.[9-20] The fuel-driven, temporal control offered by these dissipative structures allows for transient features such as catalytic activity,[21] reaction acceleration,[22,23] semiconductivity,[24] gelation,[25,26] pulsation/oscillation;[27] and evolution-like replication[28,29] or adaptation[30] to be realized. These emergent properties persist for a finite lifetime, which is determined by the amount of chemical fuel and the rate of a competing deactivation reaction that transforms the activated precursor into the lower energy form, thereby dissociating the functional state. The accumulation of spent fuel over several reaction cycles eventually hampers the operation of many dissipative systems that are driven by a continuous infusion of a chemical energy.[25,31]

Light energy provides an attractive fuel source for synthetic systems because the lack of waste production, wavelength tunability and the potential for spatial and temporal resolution affords a capability to create “living” materials with precise structural/functional control and recyclability. Light-driven dissipative systems have been developed that modulate inter-nanoparticle interactions via the action of surface-bound, photoresponsive chromophores that reversibly change their properties upon irradiation.[32-34] In contrast, the design of peptides that assemble into out-of-equilibrium structures have thus far relied on chemical reaction networks to power the formation of a metastable state.[5] Generally, high-energy molecules[18,24,26,31,35] have been used to convert a monomeric peptide precursor into a metastable derivative, with altered physico-chemical characteristics, capable of assembling into a nanostructure. However, the development of dissipative peptide assemblies driven by light energy remains as a challenge. In this work, we describe a strategy to power the dynamic assembly of a β-sheet peptide into a transient nanofiber hydrogel via the photochromic action of a spiropyran switch.

To achieve a dynamic cycle that imparted dynamic instability to the assembled structures, we conceived a peptide design capable of modulating overall amphiphilicity upon the absorption of visible light. A tetrapeptide (Fmoc-KK(SP)KF-NH_2, **1**) with a nitrospiropyran chromophore (SP) appended to a ε-amino lysine sidechain was prepared using Fmoc solid-phase

[a] *M. Liu, C. N. Creemer, T.J. Reardon, Prof. J.R. Parquette*
Department of Chemistry and Biochemistry
The Ohio State University
100 W. 18th Ave. Columbus, Ohio 43210
E-mail: parquette.1@osu.edu
† These authors contributed equally to this work.

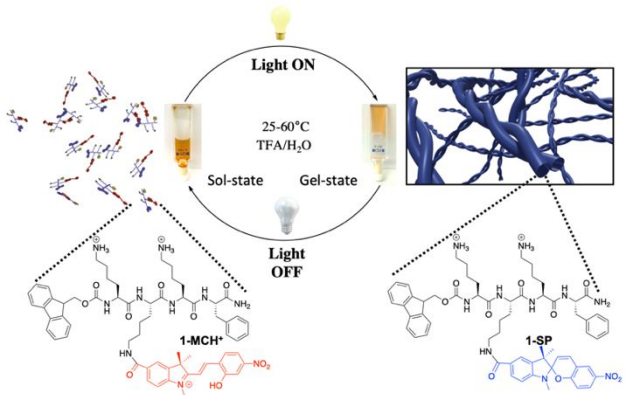

Figure 1. Transient self-assembly of nanofibers driven by visible light as fuel. Scheme of the reaction network showing interconversion between the metastable spiropyran (SP) form and the merocyanine (MCH) resting state of **1**.

chemistry (Fig. 1). The peptide sequence was constructed with alternating hydrophobic and polar residues to replicate the amphiphilic structure of β-sheet peptides.[36] In this context, the sequence contained three adjacent lysine residues in which the ε-amino position of the central lysine residue was modified with a light-responsive, spiropyran chromophore to serve as a switch to modulate the amphiphilicity of the peptide. This arrangement achieved the amphiphilic design by positioning two charged lysine side chains on one face opposite the hydrophobic phenylalanine and spiropyran side chains.

Spiropyrans constitute a well-studied group of light-switchable, photochromic dyes that reversibly interconvert between two forms with vastly different properties: a nonpolar spiropyran (SP) form and a zwitterionic, highly colored merocyanine (MC) form with a comparatively large electric dipole moment.[37] The absorption of UV light or heating causes the SP form to undergo a ring-opening reaction that produces the MC form, which returns to the SP form upon irradiation with visible light. Polar aqueous environments stabilize the zwitterionic (MC) or *O*-protonated (MCH^+) form such that thermal SP-MC isomerization often occurs spontaneously.[38] Based on these considerations, this peptide design satisfied several elements needed to impart dynamic instability into the assembly process (Fig. 1): (1) The thermodynamic resting state of the system in aqueous media was the MCH^+ form, which remained in a monomeric, unassembled state. (2) Continuous irradiation with visible light produced the metastable SP state, which achieved the amphiphilic polar/apolar sequence required for efficient β-sheet formation. (3) In the absence of continuous irradiation, the system relaxed thermally to the more stable, monomeric MCH^+ form of the peptide.

The photoresponsive behavior of **1** was initially investigated by UV-Vis spectroscopy in water with added trifluoroacetic acid (TFA). The presence of TFA induced partial ring-opening of the SP isomer during purification by HPLC, using 0.1% and 95% aq. TFA/CH_3CN as the eluant and cleavage conditions, respectively.[39] This protocol produced significant amounts (~50%) of the *O*-protonated merocyanine form (**1**-MCH^+), as evidenced by the deep yellow/orange color, the growth of a broad absorption band at 415 nm and by resolution of the isomers by analytical HPLC (Fig. S1). Irradiation of these solutions with broad-spectrum visible light (72 W, Fig. S2)

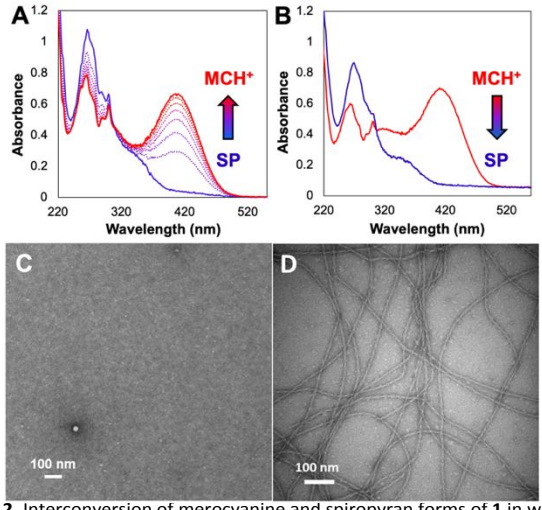

Figure 2. Interconversion of merocyanine and spiropyran forms of **1** in water (0.3 mM, 90 mM TFA), as monitored by the increase/decrease of the MCH^+ UV-Vis absorption at 415 nm. A) **1**-SP heated at 60°C in the dark and absorption recorded at 10 min. intervals over 70 min. B) Irradiation of **1**-MCH^+ with visible light for 1 min at room temperature (LED, 60 W). TEM images of **1** in water (3 mM, 90 mM TFA) C) after heating to 60°C for 60 min in the dark, D) and after irradiation with visible light for 24 h in water (3 mM, 90 mM TFA) at 60°C.

converted the **1**-MCH^+/SP mixture to the SP isomer, extinguishing the broad absorption at 415 nm within 5 min (Fig. 2). Thermal isomerization of **1**-SP to **1**-MCH^+ in water (90 mM TFA) proceeded to completion in 72 h at 37°C and within 1 h at 60°C, approximately doubling in rate for every 5°C increase in temperature (Figs. S3-4, Table S1). Although the isomerization of SP-MCH^+ was slow without at least stoichiometric amounts of TFA, an inverse rate dependence with TFA concentration was observed going from 13-180 mM, presumably due to the competitive protonation of the indolenine nitrogen at higher concentrations of TFA (Table S1).[39]

The ability of **1**-SP and **1**-MCH^+ to independently undergo self-assembly under static conditions in water was explored by transmission electron and atomic force microscopy (TEM and AFM). The presence of ambient light often produced SP/MCH^+ mixtures; therefore, solutions of **1** were thermally isomerized to **1**-MCH^+ prior to assembly experiments. Thus, an aqueous solution (3 mM, 90 mM TFA) of **1** was isomerized to **1**-MCH^+ by heating to 60°C in the dark for 1 h, then incubated for 72 h at 22°C, resulting in a yellow, free-flowing solution. TEM imaging of the sample confirmed that no discernible structures were produced by **1**-MCH^+ under these conditions (Figs. 2c, S5b). In contrast, incubating a 10 mM solution **1**-MCH^+ in water (90 mM TFA), under continuous visible light irradiation at 22°C for 72 h produced a self-supporting hydrogel (Fig. S5d). TEM imaging of the hydrogel revealed a network of twisted nanofibrils (diameter 12 ± 2 nm, pitch length 27.9 ± 2.1 nm) comprised of two smaller, intertwined fibrils (6 ± 1 nm). Fourier-transform infrared (FTIR) spectra of the hydrogel, prepared from the xerogel in D_2O (20 mM), exhibited a band at 1630 cm^{-1} characteristic of β-sheet secondary structure (Fig. S6a-b).[40] A small band at 1648 cm^{-1} in the deconvoluted spectra indicated the presence of ~12% of disordered, random coil conformation.[41] The formation of amyloid-type fibrils was confirmed using Thioflavin T (ThT), which upon binding to the **1**-SP nanofibers, experienced a strong increase in fluorescence

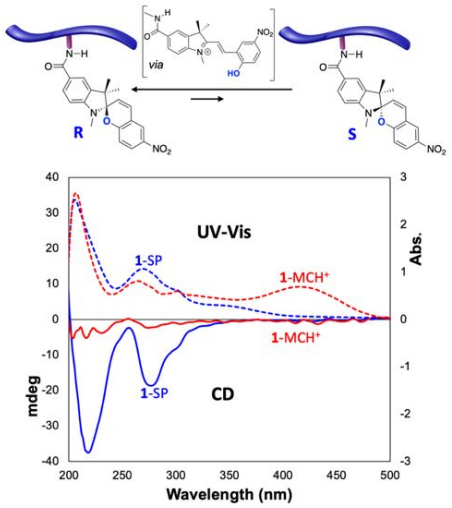

Figure 3. Rapid interconversion of R and S-spiropyran centers of **1**-SP via the intermediacy of the planar MCH⁺ form. UV-Vis and CD spectra of **1**-SP hydrogel and **1**-MCH⁺. Samples of **1**-SP or **1**-MCH⁺ were formed in water (3 mM, 90 mM TFA) at 60°C, either under continuous illumination with visible light for **1**-SP, or in the dark for **1**-MCH⁺, then diluted to 0.6 mM prior to recording the spectra.

emission intensity at ~490 nm, characteristic of amyloid structure, when excited at 450 nm(Fig. S6c).[42]

The self-assembly of **1** into the nanofiber hydrogel was then performed under continuous irradiation with visible light in water (3 mM, 90 mM TFA) at 60°C. This experiment explored the potential of **1** to undergo self-assembly in light under conditions in which **1**-SP was rapidly interconverting with the more stable MCH⁺ form, which did not form any discernible structures by TEM (Fig. 2c). At lower concentrations, these dynamic conditions (3 mM, 60°C, visible light) produced a hydrogel within minutes, in contrast with the static conditions, which often required incubating **1**-SP for several days at higher concentrations (22°C, 10 mM, visible light) for gelation to occur. Visible light irradiation efficiently isomerized a 3 mM solution of **1**-MCH⁺ to >90% **1**-SP within 5 min., even at 60°C, indicating that photochemical ring-closure could overwhelm the competing thermal ring-opening process (Figs. 2b, 4, S7). Accordingly, **1**-SP was heated at 60°C for 1 h in water (3 mM, 90 mM TFA) in the absence of light to form **1**-MCH⁺. This solution was then irradiated with visible light at 60°C for 24 h, resulting in the formation of the hydrogel that was apparent within 10 min. TEM imaging of the hydrogel formed under these dynamic conditions displayed a uniform array of twisted nanofibers with diameters of 12.3 ± 0.9 nm, a helical pitch of 27.9 ± 2.1 and AFM heights of 5.0 ± 0.5 nm. (Figs. 2d, S8-9)

The intensity of peaks in the circular dichroic (CD) spectra correlated well with the self-assembly process (Fig 3). Thus, whereas the spectrum of **1**-MCH⁺ in water (90 mM TFA) exhibited a nearly flat line, the hydrogel formed by **1**-SP showed broad negative transitions in the 220, 277 and 300-350 nm regions. Although the spiropyran chromophore was inherently chiral due to the presence of the stereogenic center at the spiro carbon, interconversion with the planar, achiral merocyanine form rapidly racemizes this center,[43] especially when the chromene ring is substituted with electron withdrawing groups.[44] Recently, chiral spiropyrans have been resolved in the solid state via dynamic enantiomeric crystallization and the

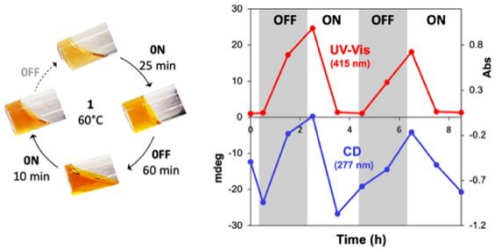

Figure 4. Temporal evolution of the assembly/disassembly cycle of **1** (3 mM) at 60°C (90 mM TFA). Formation and breakdown of the hydrogel (left) and CD and UV-Vis signals (right) at 277 and 415 nm, respectively, with each on/off cycle of visible light illumination.

resulting enantiomorphic crystals were shown to be optically and CD active.[45] The CD spectra that emerged from the assembled state of **1**-SP could be attributed to a shift in the equilibrium interconverting the R/S stereochemistry of the spiropyran center (Fig 3). The structural order and rigidity imparted by the intermolecular packing within the assembled fibers more efficiently transmits the peptide backbone chirality to the spiro center, which would shift the equilibrium to the more stable diastereomeric form. The resemblance of the CD spectrum of the assembled **1**-SP to that of the enantiopure crystals of the *R*-spiropyran[45] leads to a tentative assignment of the biased equilibrium as favoring the spiro-*R* stereochemistry.

The temporal evolution of the assembly/disassembly cycle was monitored by the formation and breakdown of the gel in conjunction with CD and UV-Vis spectroscopy. The transient nature of the assembled hydrogel permitted cycling between the soluble and hydrogel states by switching between light-off and light-on conditions, respectively. For example, as shown in Fig. 4, when **1**-MCH⁺ was dissolved in water (3 mM, 90 mM TFA) at 60°C, the system remained in a solution state. Exposure of the solution at 60°C to visible light induced the formation of a self-supporting gel within 10-30 minutes, and the system remained in the gel state for as long as the light was present. However, extinguishing the light source caused complete dissolution of the hydrogel over 30-60 min. Over eight light on/off cycles, the amplitude of the 415 nm MCH⁺ absorption decreased by ~4.7%, indicative of some photodegradation of the SP/MCH chromophore (Fig. S11).[37] The dynamic character of the gelation/dissolution cycles correlated very closely with corresponding changes in the amplitude of the 415 nm absorption in the UV-Vis spectrum, corresponding to interconversion between **1**-SP and **1**-MCH⁺, and with the amplitude of the CD ellipticity at 277 nm, indicative of the self-assembly of **1**-SP. In fact, turning the light on and off produced a progressive increase or decrease in the CD band at 277 nm that evolved on nearly the same time scale as changes in the 415 nm band, the presence/absence of nanofibers in TEM images, and with visual formation and breakdown of the gel (Figs. 4, S10). The temporal correlation of these spectral changes indicated that assembly/disassembly occurred at rates commensurate with the interconversion of **1**-SP and **1**-MCH⁺.

Trifluoroacetic acid (TFA) also played a critical role in promoting the self-assembly of **1**-SP. Attempts to achieve self-assembly/gelation under dynamic conditions (3 mM, 60°C/visible light) or static conditions (10 mM, dark) in pure water without TFA failed to induce self-assembly. Increasing the

TFA concentration progressively enhanced self-assembly plateauing at ~45 mM, as evidenced by the increase of the CD signal at 277 nm and qualitatively via TEM imaging (Figs. S12-13). Replacing TFA with acetic acid or HCl produced few, irregular aggregates rather than uniform nanofibers capable of gelation. Trifluoroacetate anions have often been used to facilitate peptide purification due to their ability to strongly ion-pair with positively charged residues, such as lysine, thereby reducing the overall hydrophilicity of the peptide.[46] These interactions significantly alter the physico-chemical properties of peptides and have been shown to affect the aggregation propensity of synthetic amyloid beta peptides.[47] The impact of TFA on the assembly could be attributed to the ability of TFA to reduce peptide hydrophilicity, which enhanced the hydrophobic driving force for the aggregation of **1**-SP. To evaluate the impact of the TFA counterion, the dynamic assembly conditions were carried out in pure water with added sodium trifluoroacetate (90 mM, 60°C, visible light), which resulted in rapid gelation and the appearance of well-formed nanofibers with similar dimensions (11.6 ± 1.2 nm in diameter; pitch of 30.1 ± 2.0 nm) to those formed with 90 mM TFA.

Conclusions. In conclusion, we have described a dynamically unstable peptide hydrogel that formed in the presence of visible light and dissipated when the light source was removed. An appended spiropyran dye reversibly converted between a nonpolar spiropyran (SP) form and polar merocyanine (MC), which mediated assembly by altering the overall amphiphilicity of the peptide. The more stable resting state of the system was the protonated MCH^+ form, which existed in a soluble, monomeric state. Exposure to visible light produced the metastable SP state, which rapidly assembled into a β-sheet hydrogel that was stable only in light. When the light was removed, the system relaxed thermally to the MCH^+form, which resulted in the dissociation of the nanofiber hydrogel. The lifetime of the hydrogel was determined by the rate of the thermal ring-opening process, which could be tuned by the amount of added TFA or temperature, varying from one hour at 60°C to three days at 37°C. The simple design of this light-driven system allows dynamical instability to be engineered into functional assemblies and reduces the production of fuel waste.

Acknowledgements. This work was supported by the National Science Foundation (CHE-2106924) and by the U.S. Army Research Laboratory and the U.S. Army Research Office under grant W911NF-14-1-0305.

Keywords: light, dissipative, peptide, self-assembly, hydrogel.

1. M. J. Webber, E. A. Appel, E. W. Meijer and R. Langer, *Nat. Mater.*, 2016, **15**, 13-26.
2. T. Shimizu, W. Ding and N. Kameta, *Chem. Rev.*, 2020, **120**, 2347-2407.
3. G. M. Whitesides, J. P. Mathias and C. T. Seto, *Science*, 1991, **254**, 1312-1319.
4. R. Freeman, M. Han, Z. Álvarez, J. A. Lewis, J. R. Wester, N. Stephanopoulos, M. T. McClendon, C. Lynsky, J. M. Godbe, H. Sangji, E. Luijten and S. I. Stupp, *Science*, 2018, **362**, 808.
5. S. Panettieri and R. V. Ulijn, *Curr. Opin. Struct. Biol.*, 2018, **51**, 9-18.
6. E. Karsenti, *Nat. Rev. Mol. Cell Bio.*, 2008, **9**, 255-262.
7. T. Le Saux, R. Plasson and L. Jullien, *Chem. Commun.*, 2014, **50**, 6189-6195.
8. B. A. Grzybowski, K. Fitzner, J. Paczesny and S. Granick, *Chem. Soc. Rev.*, 2017, **46**, 5647-5678.
9. S. A. P. van Rossum, M. Tena-Solsona, J. H. van Esch, R. Eelkema and J. Boekhoven, *Chem. Soc. Rev.*, 2017, **46**, 5519-5535.
10. E. Mattia and S. Otto, *Nat. Nanotechnol.*, 2015, **10**, 111-119.
11. S. De and R. Klajn, *Adv Mater*, 2018, **30**, e1706750.
12. B. Rieß, R. K. Grötsch and J. Boekhoven, *Chem.*, 2020, **6**, 552-578.
13. F. Della Sala, S. Neri, S. Maiti, J. L. Chen and L. J. Prins, *Curr. Opin. Biotechnol.*, 2017, **46**, 27-33.
14. J. Deng and A. Walther, *J. Am. Chem. Soc.*, 2020, **142**, 685-689.
15. S. Dhiman, A. Jain, M. Kumar and S. J. George, *J. Am. Chem. Soc.*, 2017, **139**, 16568-16575.
16. S. Maiti, I. Fortunati, C. Ferrante, P. Scrimin and L. J. Prins, *Nat. Chem.*, 2016, **8**, 725-731.
17. J. Boekhoven, W. E. Hendriksen, G. J. M. Koper, R. Eelkema and J. H. van Esch, *Science*, 2015, **349**, 1075.
18. S. Debnath, S. Roy and R. V. Ulijn, *J. Am. Chem. Soc.*, 2013, **135**, 16789-16792.
19. I. Maity, N. Wagner, R. Mukherjee, D. Dev, E. Peacock-Lopez, R. Cohen-Luria and G. Ashkenasy, *Nat. Commun.*, 2019, **10**, 4636.
20. W. A. Ogden and Z. Guan, *ChemSystemsChem*, 2019, **2**.
21. Y. Wei, S. Han, J. Kim, S. Soh and B. A. Grzybowski, *J. Am. Chem. Soc.*, 2010, **132**, 11018-11020.
22. H. Zhao, S. Sen, T. Udayabhaskararao, M. Sawczyk, K. Kucanda, D. Manna, P. K. Kundu, J. W. Lee, P. Kral and R. Klajn, *Nat. Nanotechnol.*, 2016, **11**, 82-88.
23. H. Wang, Y. Wang, B. Shen, X. Liu and M. Lee, *J. Am. Chem. Soc.*, 2019, **141**, 4182-4185.
24. M. Kumar, N. L. Ing, V. Narang, N. K. Wijerathne, A. I. Hochbaum and R. V. Ulijn, *Nat. Chem.*, 2018, **10**, 696-703.
25. N. Singh, B. Lainer, G. J. M. Formon, S. De Piccoli and T. M. Hermans, *J. Am. Chem. Soc.*, 2020, **142**, 4083-4087.
26. C. A. Angulo-Pachon and J. F. Miravet, *Chem. Commun.*, 2016, **52**, 5398-5401.
27. I. Lagzi, B. Kowalczyk, D. Wang and B. A. Grzybowski, *Angew. Chem. Int. Ed.*, 2010, **49**, 8616-8619.
28. J. M. A. Carnall, C. A. Waudby, A. M. Belenguer, M. C. A. Stuart, J. r. m. J. P. Peyralans and S. Otto, *Science*, 2010, **327**, 1502.
29. M. D. Hardy, J. Yang, J. Selimkhanov, C. M. Cole, L. S. Tsimring and N. K. Devaraj, *Proc. Natl. Acad. Sci.*, 2015, **112**, 8187.
30. J. W. Sadownik, E. Mattia, P. Nowak and S. Otto, *Nat. Chem.*, 2016, **8**, 264-269.
31. A. Sorrenti, J. Leira-Iglesias, A. Sato and T. M. Hermans, *Nat. Commun.*, 2017, **8**, 15899.
32. Z. Yin, G. Song, Y. Jiao, P. Zheng, J.-F. Xu and X. Zhang, *CCS Chemistry*, 2019, **1**, 335-342.
33. J. Palacci, S. Sacanna, A. P. Steinberg, D. J. Pine and P. M. Chaikin, *Science*, 2013, **339**, 936.
34. R. Klajn, K. J. Bishop and B. A. Grzybowski, *Proc. Natl. Acad. Sci.*, 2007, **104**, 10305-10309.
35. B. Riess, C. Wanzke, M. Tena-Solsona, R. K. Grotsch, C. Maity and J. Boekhoven, *Soft Matter*, 2018, **14**, 4852-4859.
36. X. J. Zhao and S. G. Zhang, *Chem. Soc. Rev.*, 2006, **35**, 1105-1110.
37. R. Klajn, *Chem. Soc. Rev.*, 2014, **43**, 148-184.
38. Y. Shiraishi, M. Itoh and T. Hirai, *Phys. Chem. Chem. Phys.*, 2010, **12**, 13737-13745.
39. J. T. C. Wojtyk, A. Wasey, N.-N. Xiao, P. M. Kazmaier, S. Hoz, C. Yu, R. P. Lemieux and E. Buncel, *J. Phys. Chem. A*, 2007, **111**, 2511-2516.
40. T. Miyazawa and E. R. Blout, *J. Am. Chem. Soc.*, 1961, **83**, 712-719.
41. G. W. M. Vandermeulen, K. T. Kim, Z. Wang and I. Manners, *Biomacromolecules*, 2006, **7**, 1005-1010.
42. R. Khurana, C. Coleman, C. Ionescu-Zanetti, S. A. Carter, V. Krishna, R. K. Grover, R. Roy and S. Singh, *J. Struct. Biol.*, 2005, **151**, 229-238.
43. Y. Sheng and J. Leszczynski, *Struct. Chem.*, 2013, **25**, 667-677.
44. S. Swansburg, E. Buncel and R. P. Lemieux, *J. Am. Chem. Soc.*, 2000, **122**, 6594-6600.
45. H. Ishikawa, N. Uemura, R. Saito, Y. Yoshida, T. Mino, Y. Kasashima and M. Sakamoto, *Chem. Eur. J.*, 2019, **25**, 9758-9763.
46. M. Shibue, C. T. Mant and R. S. Hodges, *J. Chromatogr. A*, 2005, **1080**, 68-75.
47. C. L. Shen, M. C. Fitzgerald and R. M. Murphy, *Biophys. J.*, 1994, **67**, 1238-1246.

